Computers in Biology and Medicine 151 (2022) 106275

Contents lists available at ScienceDirect

Computers in Biology and Medicine

journal homepage: www.elsevier.com/locate/compbiomed

Predicting mechanically ventilated patients future respiratory system elastance – A stochastic modelling approach

Christopher Yew Shuen Ang [a,*], Yeong Shiong Chiew [a,**], Xin Wang [a], Mohd Basri Mat Nor [b], Matthew E. Cove [c], J. Geoffrey Chase [d]

[a] School of Engineering, Monash University Malaysia, Selangor, Malaysia
[b] Kulliyah of Medicine, International Islamic University Malaysia, Kuantan, 25200, Malaysia
[c] Division of Respiratory & Critical Care Medicine, Department of Medicine, National University Health System, Singapore
[d] Center of Bioengineering, University of Canterbury, Christchurch, New Zealand

ARTICLE INFO

Keywords:
Mechanical ventilation
Respiratory mechanics
Patient-specific
Stochastic model
Respiratory elastance

ABSTRACT

Background and objective: Respiratory mechanics of mechanically ventilated patients evolve significantly with time, disease state and mechanical ventilation (MV) treatment. Existing deterministic data prediction methods fail to comprehensively describe the multiple sources of heterogeneity of biological systems. This research presents two respiratory mechanics stochastic models with increased prediction accuracy and range, offering improved clinical utility in MV treatment.

Methods: Two stochastic models (SM2 and SM3) were developed using retrospective patient respiratory elastance (E_{rs}) from two clinical cohorts which were averaged over time intervals of 10 and 30 min respectively. A stochastic model from a previous study (SM1) was used to benchmark performance. The stochastic models were clinically validated on an independent retrospective clinical cohort of 14 patients. Differences in predictive ability were evaluated using the difference in percentile lines and cumulative distribution density (CDD) curves.

Results: Clinical validation shows all three models captured more than 98% (median) of future E_{rs} data within the 5th – 95th percentile range. Comparisons of stochastic model percentile lines reported a maximum mean absolute percentage difference of 5.2%. The absolute differences of CDD curves were less than 0.25 in the ranges of $5 < E_{rs}$ (cmH_2O/L) < 85, suggesting similar predictive capabilities within this clinically relevant E_{rs} range.

Conclusion: The new stochastic models significantly improve prediction, clinical utility, and thus feasibility for synchronisation with clinical interventions. Paired with other MV protocols, the stochastic models developed can potentially form part of decision support systems, providing guided, personalised, and safe MV treatment.

1. Introduction

Mechanical ventilation (MV) is the primary form of support for critically ill patients with respiratory failure [1]. Existing MV treatment guidelines adopt a '*one-size-fits-all*' approach and have been primarily developed in studies of patients with acute respiratory distress syndrome (ARDS) [2–4]. This generalised treatment approach fails to account for heterogeneity across patients in terms of patient disease state and importantly, respiratory mechanics. Subsequently, it leads to some patients receiving non-optimal MV, resulting in ventilator-induced lung injury (VILI) and worsening outcomes [1,5–8]. Patient-specific respiratory mechanics evolve significantly with time, disease state, and MV treatment, ensuring optimal care does not remain so [1,9]. Therefore, the ability to capture and predict the evolving dynamics of these variables over time could aid clinicians in personalising MV treatment [10].

Existing data prediction methods, such as regression and clustering techniques are non-physiological and highly dependent on training data sets [11–13]. Furthermore, they cannot account for the heterogeneity of biological systems at the level of the individual patient and thus are not patient-specific [14,15]. In contrast, in deterministic physiological modelling, a lack of information results in model simplification, where the resulting identified parameters contain variability manifesting as system stochasticity [15]. Hence, stochastic models are required to model these intrinsic sources of heterogeneity and variability in

* Corresponding author.
** Corresponding author.
E-mail addresses: Christopher.Ang@monash.edu (C.Y.S. Ang), chiew.yeong.shiong@monash.edu (Y.S. Chiew).

https://doi.org/10.1016/j.compbiomed.2022.106275
Received 22 July 2022; Received in revised form 26 October 2022; Accepted 30 October 2022
Available online 2 November 2022
0010-4825/© 2022 Elsevier Ltd. All rights reserved.

Table 1
Patient cohorts.

Patient cohort	No. of patients	Days of recorded data	No. of recorded breaths	Age	Weight (kg)	BMI (kg/m^2)
$CARE_{01}$	24	113	2,120,834	57.00 [48.00–64.00]	65.00 [53.93–77.18]	24.75 [19.98–29.64]
$CARE_{SG}$	14	35	742,493	67.38 [54.56–70.00]	68.47 [59.40–77.17]	23.22 [22.98–23.94]
$CARE_{02}$	30	200	4,783,264	62.50 [55.00–66.00]	67.50 [60.00–78.75]	24.52 [23.00–27.88]

*Age, weight and BMI values are presented as median [interquartile range].

deterministic, physiological models [14,15].

Stochastic modelling is based on probability theory, whereby a Markov jump process is used to model biological system dynamics. Thus, unlike deterministic modelling, it allows different solutions to arise from the same input [14,15]. Stochastic models have received increased attention in describing the dynamics of biological systems [16–19], such as glycaemic control protocols in critical care [20–24]. The integration of stochastic forecasting into glycaemic control protocols produced tighter glycaemic control in 89.4% of ICU (intensive care unit) patients, while also significantly reducing hypoglycaemia episodes and ultimately reducing clinical workload [25,26]. Therefore, stochastic modelling has the potential to support personalised medicine in environments like intensive care, where heterogeneity challenges more traditional deterministic modelling approaches.

In the context of MV research, stochastic modelling has recently been investigated for predicting respiratory system elastance in respiratory failure patients [7]. Retrospective respiratory elastance values were obtained via model-based estimation and grouped into time intervals of 10 min, capturing short-term intra-patient variability. This data was used to develop and validate a stochastic model to predict future patient-specific respiratory elastance values, with 92.59% and 68.56% of the predicted values within the 90 (5th – 95th) and 50 (25th – 75th) percent ranges, respectively.

While this study demonstrates the feasibility of stochastic modelling in MV care, its clinical utility is limited. In particular, this stochastic model was trained with data from a single cohort of only 24 patients, and clinical validation was limited because it was performed on patients from the same cohort. Moreover, the selected proof-of-concept interval size of 10 min would not be feasible for application in critical care as it would lead to a significant increase in clinician workload [27].

Respiratory elastance plays an important role in representing respiratory system function and the progression of patient-specific disease states [28]. It is defined as a measure of the elastic properties of the respiratory system which includes the lungs and chest wall [29,30]. A patient's respiratory elastance is typically measured using an end-inspiratory pause or by using model-based methods [9,28,31–35]. Measurements of respiratory elastance are also important for guiding the selection of MV settings. Suter et al. investigated the selection of positive end-expiratory pressure, PEEP based on respiratory compliance (inverse of elastance) [36]. In this study, the authors reported that the selection of PEEP at the highest compliance (or lowest respiratory elastance) also resulted in maximum oxygen delivery and lowest dead-space fraction. Other studies on respiratory elastance have also been carried out, suggesting that elastance can be used to guide MV settings [37,38]. In certain ARDS (acute respiratory distress syndrome) phenotypes, a physiologic approach of elastance-based PEEP titration may lead to better patient outcomes as compared to oxygenation-based PEEP strategies [39].

This research presents respiratory mechanics stochastic models with increased prediction accuracy by using patient data from two different patient cohorts. Increasing training data provides a wider, more clinically complete respiratory elastance prediction range. An interval of 30 min bridges the gap between simulation and practical clinical utility. Finally, this study provides more extensive clinical validation of the extended stochastic model based on the work of Lee et al. [7] using data from an independent patient cohort. The end result is more robust, clinically more relevant and applicable, creating the potential for personalised real-time MV care.

2. Methodology

2.1. Clinical patient data

This study uses measured airway pressure and flow data from 68 retrospective patients across three clinical cohorts receiving invasive MV for respiratory failure [32,40]. The three cohorts (ethics approval)

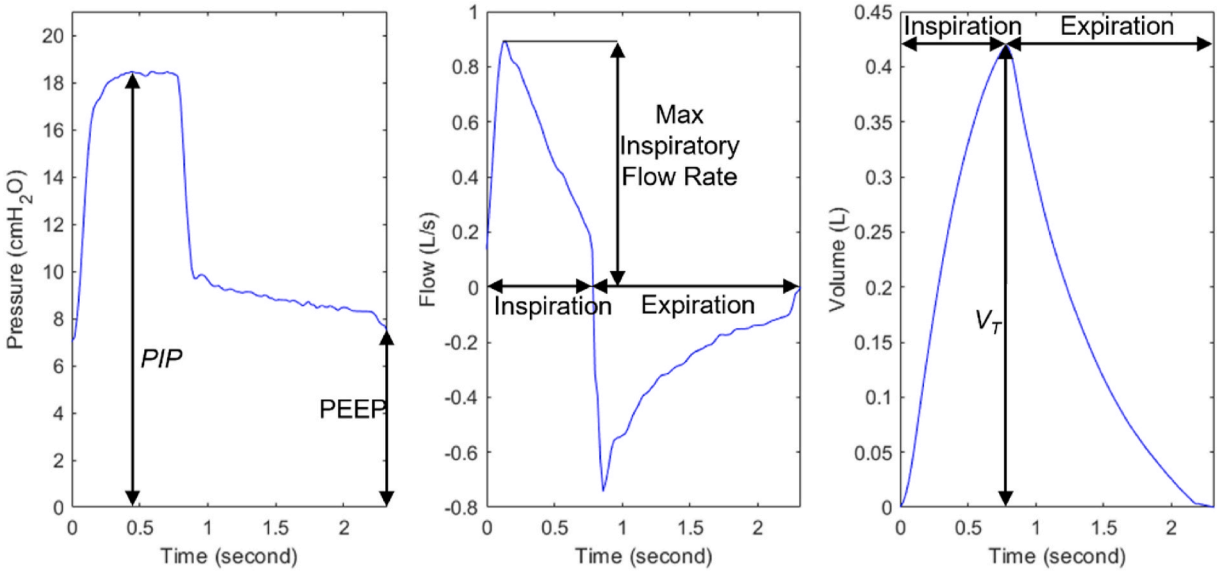

Fig. 1. A typical respiration pressure (left), flow (middle), and volume (right) waveform. PIP is the peak inspiratory flow, PEEP is the positive end-expiratory pressure, and V_T is the tidal volume. The inspiration and expiration portions of the breath are also shown as well as the maximum inspiratory flow rate.

are denoted: **1**) $CARE_{01}$ (Ref: IIUM/504/14/11/2/IREC 666); **2**) $CARE_{SG}$ (DSRB Ref:2018/00042); and **3**) $CARE_{02}$ (Ref: IIUM/504/14/11/2/IREC 2020–100). Details are shown in Table 1.

Ventilator data was recorded using a MV data acquisition system connected to a Puritan Bennett 980 ventilator (Covidien, Boulder, CO, USA) [41,42]. Mechanical ventilation airway pressure (cmH_2O) and flow (L/min) were recorded at a sampling rate of 50 Hz. Each breathing cycle is separated and filtered to remove small data fluctuations and to ensure completeness of individual breaths. Filtering criteria are defined for each breath [7,33]. Each breath must have the following:

- The start of inspiration is defined as the first overall increase in flow rate (greater than 0.1 L/s) and pressure (2 cmH_2O above positive end-expiratory pressure, PEEP). Data is checked over the next 8 data points (0.16 s) to ensure constant positive flow.
- The start of expiration is defined as the first overall decrease in flow rate (less than −0.1 L/s). Data is checked over the next 8 data points (0.16 s) to ensure constant negative flow.
- Peak Inspiratory Volume (PIV) reaches or exceeds approximately 10% of a typical tidal volume (40 mL).
- Peak Inspiratory Pressure (PIP) is of significant value (PIP > (PEEP + 1 cmH_2O), where typical PIP is approximately 10–14 cmH_2O above PEEP.
- Maximum flow rate exceeds 6 L/min.
- Expiration is detected within 4.125 s of the calculated onset of inspiration as defined above.
- Asynchronous breaths are filtered [7,33].

A typical respiratory pressure, flow and volume waveform is shown in Fig. 1. Furthermore, MV settings and parameters such as positive end-expiratory pressure, PEEP; peak inspiratory pressure, PIP; tidal volume, V_T; inspiratory to expiratory ratio, I:E ratio; respiration rate, RR; minute ventilation, and the maximum inspiratory flow of each breath are recorded [1]. A Kruskal-Wallis one-way analysis of variance test is also performed to determine if the ventilator settings and parameters are significantly different between the three patient cohorts.

2.2. Stochastic model development

Stochastic modelling is used to approximate potential outcomes for a process showing stochasticity, where probability densities can be created by recording stochastic variables as a function of time [7]. In this research, respiratory elastance derived from a single compartment lung model is used for the stochastic model development. Lung condition and response to MV can be characterised using this respiratory mechanics model [29,43,44]:

$$P_{aw}(t) = E_{rs}V(t) + R_{rs}\dot{V}(t) + P_o \tag{1}$$

Where P_{aw} is the airway pressure (cmH_2O), t is the time, E_{rs} is the respiratory elastance of a single breath (cmH_2O/L), V is the volume (L), R_{rs} is the respiratory resistance of a single breath (cmH_2Os/L), $\dot{V}$ is the airflow (L/s), P_o is the offset pressure or PEEP (cmH_2O) when there is no auto-PEEP.

Using airway pressure and flow data obtained from the ventilator, **(1)** can be solved for E_{rs} and R_{rs} using integral-based parameter identification from the equation defined:

$$\int P_{aw}(t)\,dt = E_{rs}\int V(t)\,dt + R_{rs}\int \dot{V}(t)\,dt + \int P_o\,dt \tag{2}$$

Where the use of integrals significantly increases robustness to noise [32,43,45].

For each patient cohort, E_{rs} and R_{rs} for all breaths are identified and recorded. A Kruskal-Wallis one-way analysis of variance test is performed to determine if the identified respiratory mechanics (E_{rs} and R_{rs}) are significantly different between the patient cohorts.

E_{rs} is identified and recorded for all patient breaths, and are averaged into mean values over set time intervals, $E_{rs\,N}$, where N is a selected time interval. In this study, N is chosen as 10 and 30 min. The mean E_{rs} data are sorted into data pairs of $E_{rs\,N}$ and $E_{rs\,N+1}$, which are the mean respiratory elastance values of the current N-minute interval and the subsequent N-minute interval, respectively. The sorted data pairs obtained from the patient cohorts form the basis of the stochastic model [7].

The stochastic model based on a two-dimensional kernel density estimation (KDE) method is used as the distribution of $E_{rs\,N+1}$ varies with $E_{rs\,N}$, and cannot be described using standard statistical distributions [7,21]. The variations in $E_{rs\,N}$ can be described as a Markov jump process, where the conditional probability density function of future $E_{rs\,N}$ values depends only upon the current $E_{rs\,N}$ value. The conditional probability density of $E_{rs\,N+1} = y$ given the value of $E_{rs\,N} = x$ can be described using the Bayes Theorem:

$$P\left(E_{rs,N+1} = y \middle| E_{rs,N} = x\right) = \frac{P\left(E_{rs,N+1} = y, E_{rs,N} = x\right)}{P\left(E_{rs,N} = x\right)} = \frac{\alpha_i}{\beta_i} \tag{3}$$

A conditional probability function can be used to describe future values of $E_{rs\,N}$ which can be calculated using KDE [46]:

$$\alpha_i = P(x,y) = \frac{1}{n}\sum_{i=1}^{n} \frac{\varnothing\left(x; x_i, \sigma_{x_i}^2\right)}{p_{x_i}} \frac{\varnothing\left(y; y_i, \sigma_{y_i}^2\right)}{p_{y_i}} \tag{4}$$

Where α_i is the 2-dimensional kernel density estimated joint probability density function, P(x,y), and is defined by the fitted values of E_{rs} data pairs with coordinates x_i and y_i. The terms $\varnothing(x; x_i, \sigma_{x_i}^2)$ and $\varnothing(y; y_i, \sigma_{y_i}^2)$ represent the normal probability distribution function centered at individual data points of x_i and y_i, with $\sigma_{x_i}^2$ and $\sigma_{y_i}^2$ being the square of the variances, yielding:

$$p_{x_i} = \int_0^\infty \varnothing\left(x; x_i, \sigma_{x_i}^2\right) \tag{5}$$

$$p_{y_i} = \int_0^\infty \varnothing\left(y; y_i, \sigma_{y_i}^2\right) \tag{6}$$

Putting **(5)** and **(6)** in **(4)** ensures that the probability distributions are normalised in the positive domain, thus enforcing physiological validity with non-negative E_{rs} values. β_i can be calculated by integrating **(4)** with respect to y:

$$\beta_i = \int P(x,y)dy = \frac{1}{n}\sum_{i=1}^{n} \frac{\varnothing\left(x; x_i, \sigma_{x_i}^2\right)}{p_{x_i}} \int \frac{\varnothing\left(y; y_i, \sigma_{y_i}^2\right)}{p_{y_i}} dy = \frac{1}{n}\sum_{i=1}^{n} \frac{\varnothing\left(x; x_i, \sigma_{x_i}^2\right)}{p_{x_i}} \bullet 1 \tag{7}$$

Thus, **(3)** can be expressed as:

$$P\left(E_{rs,N+1} = y \middle| E_{rs,N} = x\right) = \frac{\sum_{i=1}^{n} \frac{\varnothing\left(x; x_i, \sigma_{x_i}^2\right)}{p_{x_i}} \frac{\varnothing\left(y; y_i, \sigma_{y_i}^2\right)}{p_{y_i}}}{\sum_{i=1}^{n} \frac{\varnothing\left(x; x_i, \sigma_{x_i}^2\right)}{p_{x_i}}} \tag{8}$$

Where **(8)** defines the two-dimensional KDE for the conditional variation of E_{rs}, where E_{rs} depends on its prior state.

This approach allows the probability of E_{rs} at the time interval N+1 ($E_{rs\,N+1} = y$) to be calculated given E_{rs} at time point N ($E_{rs\,N} = x$) is known. Detailed steps for calculating $P(y|x)$ are described by Lin et al. [20]. In addition, the variance estimators (i.e., σ_x and σ_y) are multiplied with a constant c, which effectively adjusts the kernel bandwidth and the degree of smoothing over the data [22]. To ensure comparability with the stochastic model previously developed by Lee et al. (SM1), this constant was set to a value of 1. The result is a 3-dimensional stochastic model of E_{rs} variability. The percentile lines represent the probability interval of future $E_{rs\,N+1}$ values, which can be used to assess the potential

Table 2
Stochastic model parameters, where training data sets are defined demographically in Table 1.

Stochastic Model Name	SM1	SM2	SM3
Time Interval, *N* (Minutes)	10	10	30
Training Dataset (Patient Cohort)	$CARE_{01}$	$CARE_{01}$, $CARE_{02}$	$CARE_{01}$, $CARE_{02}$
No. of Patients	24	54	54
No. of Days	113	313	313
No. of Initial Breaths	2,120,834	6,904,098	6,904,098
No. of Remaining Breaths After Filtering (Percentage, %)	1,699,401 (80.13)	5,589,339 (80.96)	5,589,339 (80.96)
No. of E_{rs} pairs	10,213	28,397	7,146

and risk of changes in MV settings and care. In this study, three different stochastic models are developed using different training datasets and time intervals, all of which are detailed in Table 2.

2.3. Validation of stochastic models

The developed stochastic models require self-validation, cross-validation, and clinical validation to provide a comprehensive assessment of the model's performance. For model self-validation, the developed stochastic models are used to generate probability intervals of potential E_{rs} values ($E_{rs\ N+1\ sim}$) over the range of identified $E_{rs\ N}$ values. The actual $E_{rs\ N+1}$ measurements are then compared to the predicted $E_{rs\ N+1\ sim}$ probability intervals. The testing and training data are the same, providing a best-case estimate.

A 5-fold cross-validation is also performed to evaluate model robustness [7,24]. The training dataset is divided into 5 approximately equisized sets of data pairs, 4 of which are used to develop the stochastic model, and the remaining set is used as test data. Data in the test sets of each validation fold are unique and non-repeating. In each validation fold, each E_{rs} from the test dataset is used to predict $E_{rs\ N+1}$ probability intervals. The percentage of actual $E_{rs\ N+1}$ values that are within the model-predicted 25th – 75th and 5th – 95th percentile range are compared to the ideal values of 50% and 90%, respectively. Results showing less deviation from the ideal values indicate good model prediction performance. Low variation in the cross-validation outcomes would indicate data sufficiency and model robustness. This cross-validation process is performed on all three stochastic models.

In addition, model performance is evaluated using retrospective patient data for clinical validity. Similar methods of validation have been presented in prior stochastic modelling studies [22,24]. Each of the three developed stochastic models is used to analyse patients from the $CARE_{SG}$ cohort. The stochastic models are used to predict the range of future $E_{rs\ N+1}$ values and then compared to the actual $E_{rs\ N+1}$ values.

The percentage of actual patient $E_{rs\ N+1}$ values falling within the stochastic model predicted 25th – 75th and 5th – 95th percentile range are analysed. For each patient, only the first 12 h of patient data are analysed to ensure consistency and comparability across cohorts. Patient

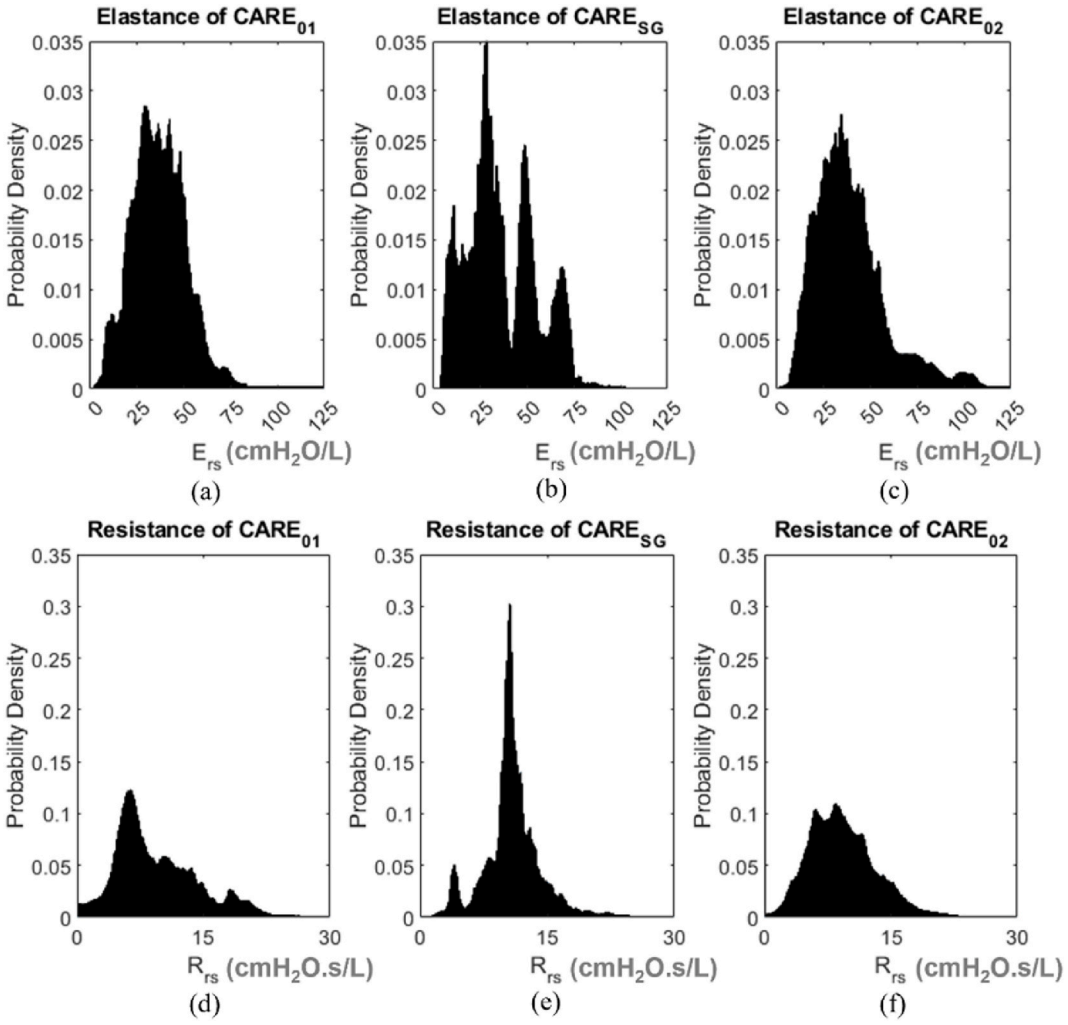

Fig. 2. Histogram showing the probability density of E_{rs} of patient cohorts: $CARE_{01}$ (a), $CARE_{SG}$ (b), and $CARE_{02}$ (c). The probability density of R_{rs} of patient cohorts: $CARE_{01}$ (d), $CARE_{SG}$ (e), and $CARE_{02}$ (f).

Table 3
Respiratory mechanics and ventilator parameters of the patient cohorts, where all settings are statistically significantly different ($p < 0.05$) between cohorts except for tidal volume (V_T).

Patient Cohort	$CARE_{01}$	$CARE_{SG}$	$CARE_{02}$
E_{rs} (cmH_2O/L)	36.95 [27.51–47.40]	33.11 [23.59–50.21]	36.51 [26.31–48.66]
R_{rs} (cmH_2O.s/L)	7.93 [5.55–12.51]	10.70 [9.55–12.34]	8.82 [6.29–11.68]
PEEP (cmH_2O)	9.00 [7.50–10.00]	8.00 [7.50–10.00]	9.00 [6.00–13.00]
PIP (cmH_2O)	23.06 [20.01–28.47]	24.39 [20.80–28.69]	28.13 [19.66–31.17]
V_T (L)	0.36 [0.31–0.44]	0.37 [0.31–0.44]	0.38 [0.35–0.45]
I:E ratio	0.53 [0.44–0.76]	0.57 [0.46–0.79]	0.49 [0.43–0.68]
Respiration rate (breaths/min)	20.83 [16.13–26.79]	22.22 [17.34–30.30]	25.21 [20.55–35.29]
Minute Ventilation (L/min)	8.25 [6.69–9.92]	9.35 [7.39–11.66]	10.57 [8.90–12.37]
Max Inspiratory Flow (L/s)	0.76 [0.55–0.96]	0.95 [0.72–1.17]	0.98 [0.81–1.11]

*Results are reported as values of median [Interquartile range, IQR].

data are processed and sorted into time intervals, N, corresponding to each stochastic model. The median absolute percentage error (MAPE) of model fitting is also calculated:

$$MAPE = Median\left|\frac{P_{Sim} - P_{Actual}}{P_{Sim}} \times 100\%\right| \tag{9}$$

Where P_{Sim} is the pressure waveform forward simulated using the identified respiratory mechanics from **(2)** and P_{Actual} is the actual pressure waveform obtained from the ventilator. It is assumed that the change in E_{rs} is solely due to the evolution of the patient's respiratory system condition, rather than the change in PEEP. Therefore, patient PEEP levels are also recorded throughout the duration of ventilation.

2.4. Comparison of stochastic models

SM1 is a stochastic model developed using data from a previous study by Lee et al. [7] and is the benchmark model. SM2 combines both $CARE_{01}$ and $CARE_{02}$ to form a bigger patient dataset. Finally, SM3 uses a larger time interval of 30 min with the same training set as SM2. These details are shown in Table 2.

To compare the predictive abilities of the 3 stochastic models, the mean absolute percentage difference (MAPD) between each percentile (5th, 25th, 50th, 75th, and 95th) is calculated:

$$MAPD = \frac{1}{K}\sum_{i=1}^{K}\left|\frac{SM_a - SM_b}{\frac{SM_a + SM_b}{2}}\right| \times 100\% \tag{10}$$

Where K is the total number of data points along the $E_{rs\ N}$ axis. SM_a and SM_b are the two stochastic models used for this analysis.

Further, using each stochastic model, the generated conditional probability density (CPD) curve is converted to a cumulative distribution density (CDD) curve. Each slice of the surface along the $E_{rs\ N+1}$ axis has an area under the curve summing to 1. The stochastic models will be compared by calculating the absolute difference between the CDD plots:

$$Absolute\ difference = \left|SM_{a,x,y} - SM_{b,x,y}\right| \tag{11}$$

Where x and y represent coordinates of individual data points along the $E_{rs\ N}$ and $E_{rs\ N+1}$ axis, respectively.

Regions of high absolute difference are defined as regions with an absolute difference greater than the arbitrarily selected threshold value of 0.25. The percentage difference of the total area under the curve (AUC) of the absolute difference plots, PD_{AUC} are also calculated:

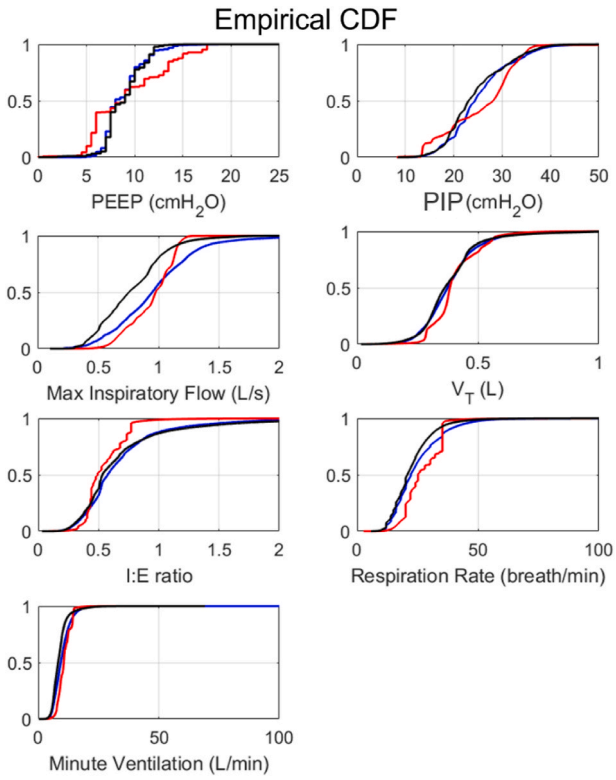

Fig. 3. The CDF plots of MV settings and parameters of the patient cohorts: $CARE_{01}$ (black), $CARE_{SG}$ (red), and $CARE_{02}$ (blue).

$$PD_{AUC} = \frac{AUC\left(\left|SM_{a,x,y} - SM_{b,x,y}\right|\right)}{AUC\left(\frac{SM_{a,x,y} + SM_{b,x,y}}{2}\right)} \times 100\% \tag{12}$$

This metric describes the average percentage difference per data point between two stochastic models across the entire range of $E_{rs\ N}$. To ensure comparability, the limits of the $E_{rs\ N}$ axis used in the analyses above are limited from 5 to 125 cmH_2O. Similar validation methods have been used to analyse blood glucose and insulin sensitivity stochastic models [47].

3. Results

3.1. Patient cohort and stochastic models

The probability densities of E_{rs} and R_{rs} of all three patient cohorts are presented in Fig. 2. The E_{rs} and R_{rs} values used for all three patient cohorts are presented in Table 3. While the E_{rs} ranges are similar, the distributions of the identified respiratory mechanics are very different for all three cohorts ($P < 0.05$; Kruskal-Wallis). The E_{rs} pairs used to develop SM1, SM2 and SM3 have a median [interquartile range] E_{rs} value of 35.80 [26.22–45.27] cmH_2O/L, 34.62 [24.94–45.46] cmH_2O/L, and 34.73 [25.15–45.34] cmH_2O/L, respectively. The cumulative distribution density (CDF) plots of the overall MV settings and parameters of each patient cohort are presented in Fig. 3. A summary of all ventilator settings and parameters such as PEEP, PIP, V_T, I:E ratio, minute ventilation, respiration rate, and maximum inspiratory flow are also presented in Table 3. These ventilator settings and parameters are significantly different between the patient cohorts ($P < 0.05$; Kruskal-Wallis), except for V_T, which is not significantly different between the $CARE_{01}$ and $CARE_{SG}$ cohort, where this result is unsurprising as setting a tidal volume (V_T) range to 6–8 ml/kg is one of the few well-accepted MV care guidelines [1,48,49].

The left column of Fig. 4 shows the conditional probability density

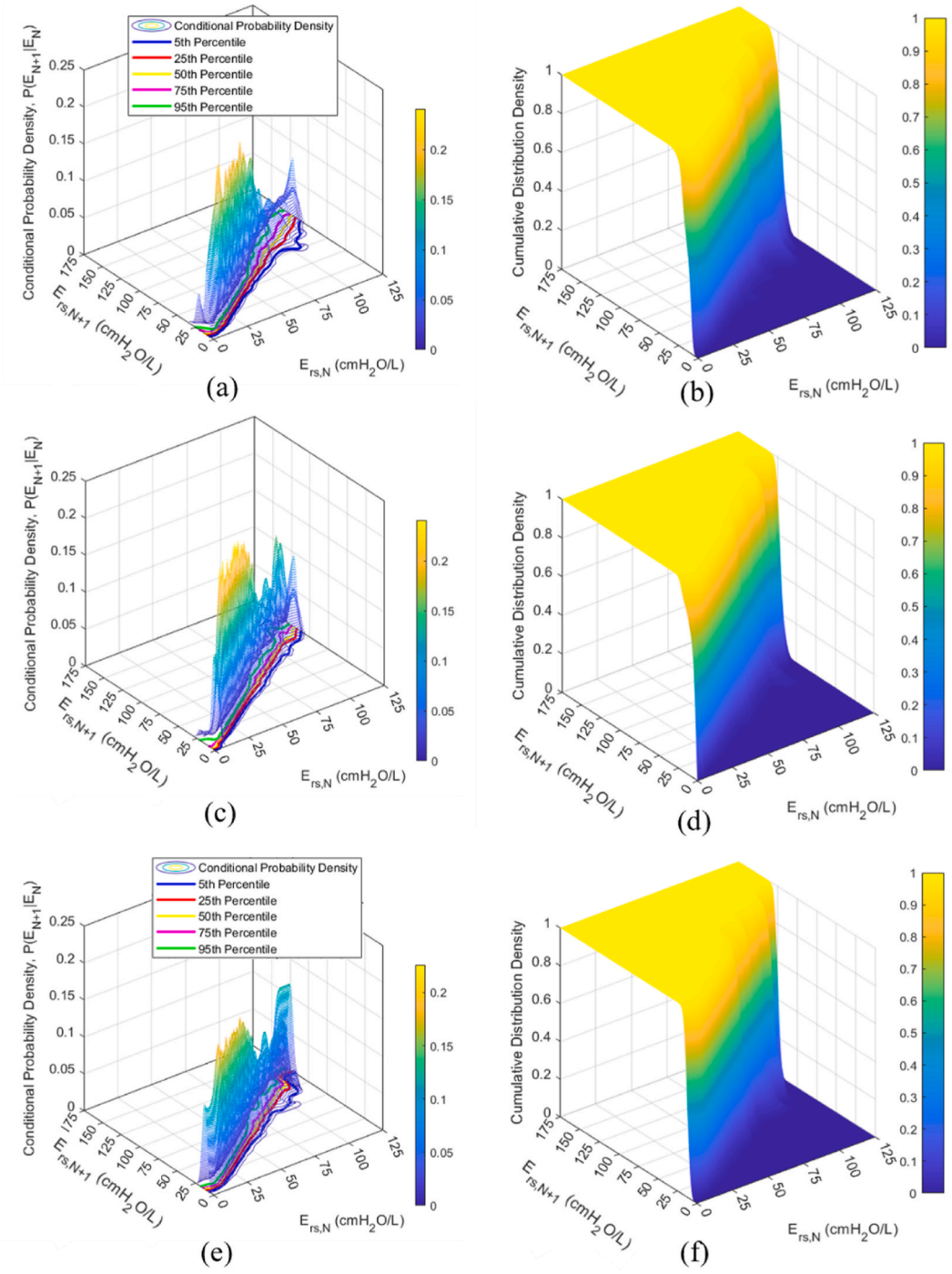

Fig. 4. The conditional probability density (left column) and cumulative distribution density (right column) corresponding to SM1, SM2, and SM3, respectively (from top to bottom).

(CPD) created from each training dataset. The corresponding cumulative distribution density (CDD) plots are shown in Fig. 4 **(right column)**. The resulting stochastic models of E_{rs} along with the percentile lines are shown in Fig. 5 **(left column)**. Self-validation results of each stochastic model are presented graphically in Fig. 5 **(right column)**, and the percentage of actual $E_{rs\ N+1}$ values within the stochastic model-predicted 25th – 75th and 5th – 95th percentile ranges are shown in Table 4. Table 5 presents the results of the 5-fold cross-validation of each stochastic model. In all cases, self-validation and cross-validation show ~68% of data within the 25th – 75th percentile range and ~92% of the data within the 5th – 95th percentile range.

3.2. Clinical validation

The independent $CARE_{SG}$ cohort yielded predicted $E_{rs\ N+1}$ ranges for the 25th – 75th and 5th – 95th percentile ranges as shown in Table 6. For both SM1 and SM2, the stochastic models conservatively captured more than 90% of the data within the 5th – 95th percentile range. For SM3 with a longer time interval and lesser data pairs (Table 2), 2 patients of the $CARE_{SG}$ cohort had less than 90% of the data within the 5th – 95th percentile range.

$E_{rs\ N+1}$ predictions, PEEP levels, and MAPE of these Patients 3 and 10 from the $CARE_{SG}$ cohort using the 3 stochastic models are shown in

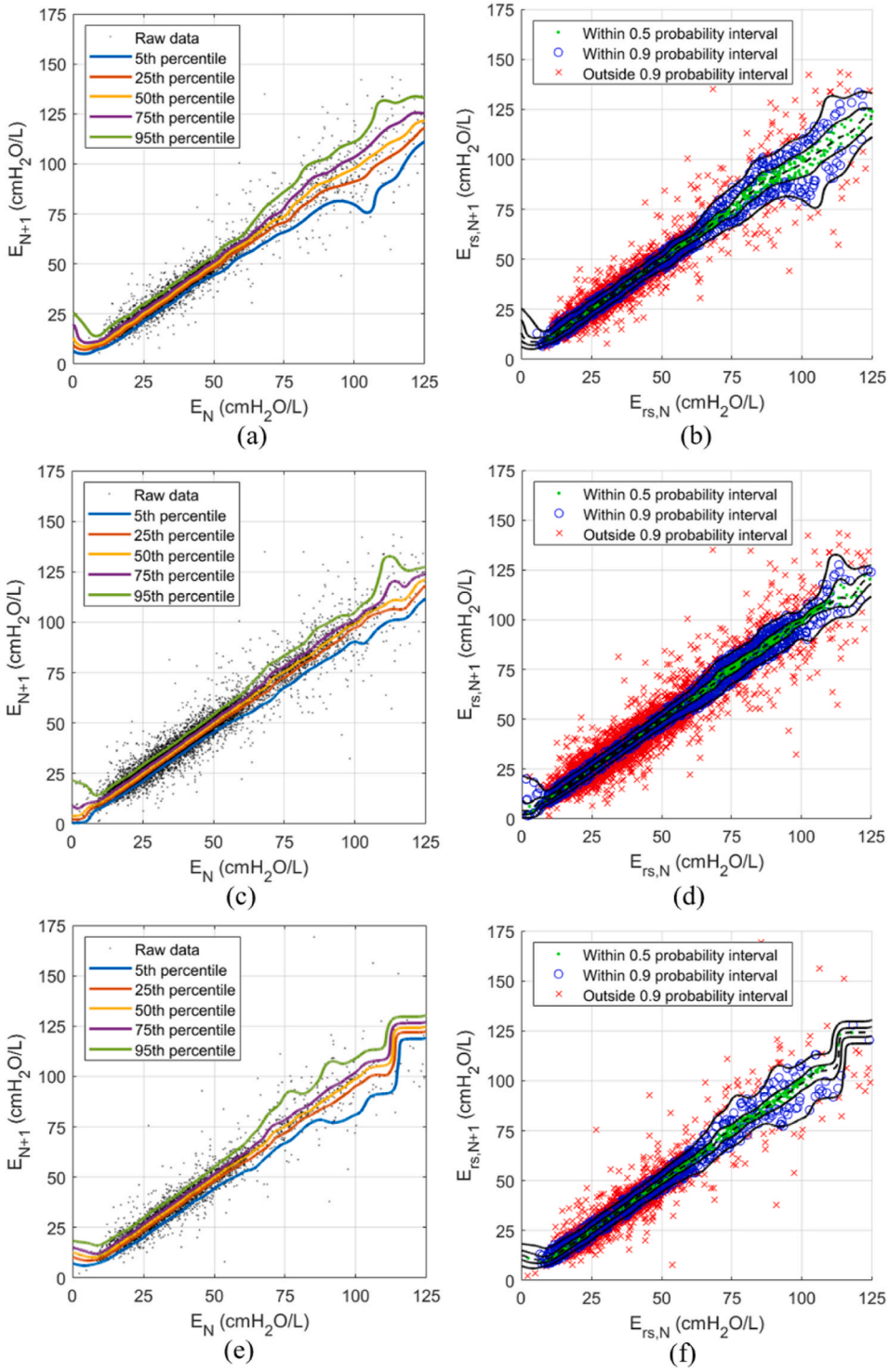

Fig. 5. The developed stochastic models (left column) and self-validation results (right column) corresponding to SM1, SM2, and SM3, respectively (from top to bottom). The 0.5 and 0.9 probability interval corresponds to the 25th – 75th and 5th – 95th percentile range, respectively.

Table 4
Self-validation of stochastic models, where Pass50 and Pass90 are the percentage (%) of actual $E_{rs,N+1}$ values within the stochastic model-predicted 25th – 75th and 5th – 95th percentile range, respectively.

Stochastic Model	SM1	SM2	SM3
Within 25th to 75th percentile (Pass50)	67.90	66.97	67.27
Within 5th to 95th percentile (Pass90)	92.84	92.54	92.44

Figs. 6 and 7, respectively. The first 12 h of patient data are analysed, giving a total of 72 intervals (per patient) analysed for SM1 and SM2, while SM3 has a total of 24 intervals (per patient) analysed with its longer interval.

3.3. Comparison of stochastic models

The mean absolute percentage difference (MAPD) of percentiles when comparing two different stochastic models is shown in Table 7.

Table 5
5-fold cross-validation of stochastic models where each 20% block of data for training (80% or 4 blocks) and testing (20% or 1 block) are denoted "a", "b", "c", "d", and "e" to show which 4 are used in training. The block left out of the training set is used for testing in 5-fold cross-validation.

Stochastic Model	SM1		SM2		SM3	
Training Datasets[c]	**Pass50**[a]	**Pass90**[a]	**Pass50**	**Pass90**	**Pass50**	**Pass90**
[-,b,c,d,e]	52.34	71.52	65.73	87.90	65.27	87.48
[a,-,c,d,e]	66.92	93.37	64.67	92.54	66.89	92.59
[a,b,-,d,e]	75.28	95.66	69.59	93.06	67.39	92.97
[a,b,c,-,e]	78.22	96.79	74.60	95.08	76.55	95.04
[a,b,c,d,-]	65.07	92.30	66.61	93.22	66.55	93.24
Mean (Standard Deviation)	67.57 (±10.15)	89.93 (±10.44)	68.24 (±4.00)	92.36 (±2.67)	68.53 (±4.55)	92.26 (±2.84)
Percentage difference (%)[b]	0.50	3.14	1.89	0.20	1.88	0.19

[a] Pass50 and Pass90 are the percentage (%) of actual $E_{rs,N+1}$ values within the stochastic model-predicted 25th – 75th and 5th – 95th percentile range, respectively.
[b] Percentage difference is the absolute percentage difference (%) of the mean Pass50 or Pass90 with respect to the self-validation results (Table 2).
[c] For the stochastic model training datasets, **[-,b,c,d,e]** indicates that **subsets b,c,d** and **e** were used for training, whereas **subset a** was used as the validation set, and so forth.

Table 6
$E_{rs,N+1}$ predictions for each stochastic model, where the 50 and 90 prc interval corresponds to the 25th – 75th and 5th – 95th percentile range, respectively, IQR is inter-quartile range, and values are reported as percentages (%).

	SM1			SM2			SM3		
Patient	Within 50 prc interval	Within 90 prc interval	Outside 90 prc interval	Within 50 prc interval	Within 90 prc interval	Outside 90 prc interval	Within 50 prc interval	Within 90 prc interval	Outside 90 prc interval
1	22.54	98.59	1.41	26.76	98.59	1.41	13.04	100.00	0.00
2	88.73	100.00	0.00	81.69	97.18	2.82	73.91	95.65	4.35
3	64.79	98.59	1.41	60.56	95.77	4.23	47.83	100.00	0.00
4	73.24	97.18	2.82	70.42	94.37	5.63	65.22	100.00	0.00
5	90.14	98.59	1.41	80.28	98.59	1.41	91.30	100.00	0.00
6	88.73	100.00	0.00	91.55	100.00	0.00	82.61	100.00	0.00
7	63.38	95.77	4.23	60.56	94.37	5.63	52.17	86.96	13.04
8	78.87	100.00	0.00	71.83	100.00	0.00	60.87	100.00	0.00
9	87.32	100.00	0.00	84.51	100.00	0.00	82.61	100.00	0.00
10	74.65	91.55	8.45	74.65	92.96	7.04	52.17	78.26	21.74
11	77.46	97.18	2.82	76.06	97.18	2.82	73.91	100.00	0.00
12	91.55	100.00	0.00	90.14	100.00	0.00	91.30	100.00	0.00
13	85.92	100.00	0.00	83.10	100.00	0.00	82.61	100.00	0.00
14	78.87	98.59	1.41	76.06	98.59	1.41	73.91	95.65	4.35
Median	78.87	98.59	1.41	76.06	98.59	1.41	73.91	100	0.00
[IQR]	[73.59–88.38]	[97.54–100]	[0.00–2.46]	[70.77–82.75]	[96.13–100]	[0.00–3.87]	[54.35–82.61]	[96.74–100]	[0.00–3.26]
Mean	76.16	98.29	1.71	73.44	97.69	2.31	67.39	96.89	3.11

Results show that there is a relatively higher MAPD between the 5th and 95th percentiles. The absolute differences between the cumulative distribution density (CDD) plots of the stochastic models are also shown in Fig. 8. The percentage difference of the total area under the curve of the absolute difference plots, PD_{AUC} are 1.16%, 1.46% and 1.15% for SM1-SM2, SM1-SM3, and SM2-SM3, respectively.

4. Discussion

4.1. Stochastic models

Fig. 3 shows that the MV settings and parameters used are different for all three patient cohorts ($CARE_{01}$, $CARE_{02}$ and $CARE_{SG}$), except for V_T, which is not significantly different between the $CARE_{01}$ and $CARE_{SG}$ cohorts. PEEPs used for $CARE_{SG}$ cohort had slightly wider ranges, whereas maximum inspiratory flows for $CARE_{01}$ were lower. The I:E ratio and respiration rate of the $CARE_{SG}$ cohort also have slightly narrower ranges compared to the $CARE_{01}$ and $CARE_{02}$ cohorts. The results in Table 3 show the variation of respiratory mechanics as well as ventilator settings and parameters, which are all shown to be significantly different between cohorts, apart from V_T of the $CARE_{01}$ and $CARE_{SG}$ cohort ($P < 0.05$; Kruskal-Wallis). This result indicates the different centers have different clinical practices and preferences. Table 2 shows the training dataset composition of each stochastic model in this study. Used as part of the training data for stochastic models SM2 and SM3, the addition of the $CARE_{02}$ patient cohort increases the total number of filtered breaths by an additional 229% in comparison to the original training dataset ($CARE_{01}$) used by Lee et al. [7]. Subsequently, the amount of training data (E_{rs} pairs) available is increased by an additional 178% for SM2. This increase in training data would ensure that the developed stochastic models are more inclusive and capable of statistically representing a wider range of patient conditions as compared to SM1. Despite using the same breath dataset as SM2, the training dataset for SM3 only consisted of 7,146 E_{rs} pairs, mainly due to the selection of a longer 30-min time interval, N.

From Table 3, median E_{rs} values of $CARE_{SG}$ differ from the $CARE_{01}$ and $CARE_{02}$ cohorts by 3.84 and 3.40 cmH_2O/L, respectively, suggesting patients in the validation dataset have dissimilar and varying respiratory mechanics profiles as shown in Fig. 2, and are thus suitable for validation analysis. The E_{rs} values of the three patient cohorts are significantly different while falling within physiological ranges reported by literature [3,30,50–52]. Both $CARE_{01}$ and $CARE_{02}$ exhibit a non-normal distribution that is skewed towards the right, suggesting that there are lesser patients with high respiratory elastance and resistance. The respiratory elastance distribution of both cohorts is centered at the interquartile range (25th and 75th percentile) of ~25–50 cmH_2O/L, indicating that large patient samples of respiratory elastance are within this range. $CARE_{SG}$ displayed a trimodal distribution. This distribution is likely due to the difference in cohort patient numbers where the $CARE_{SG}$ cohort consists of only 14 patients, thus leading to the difference in data distributions. This further highlights the need for multi-center observational trials for continuous respiratory mechanics monitoring and the development of the stochastic model.

The left column (a,c,e) in Fig. 4 shows the conditional probability

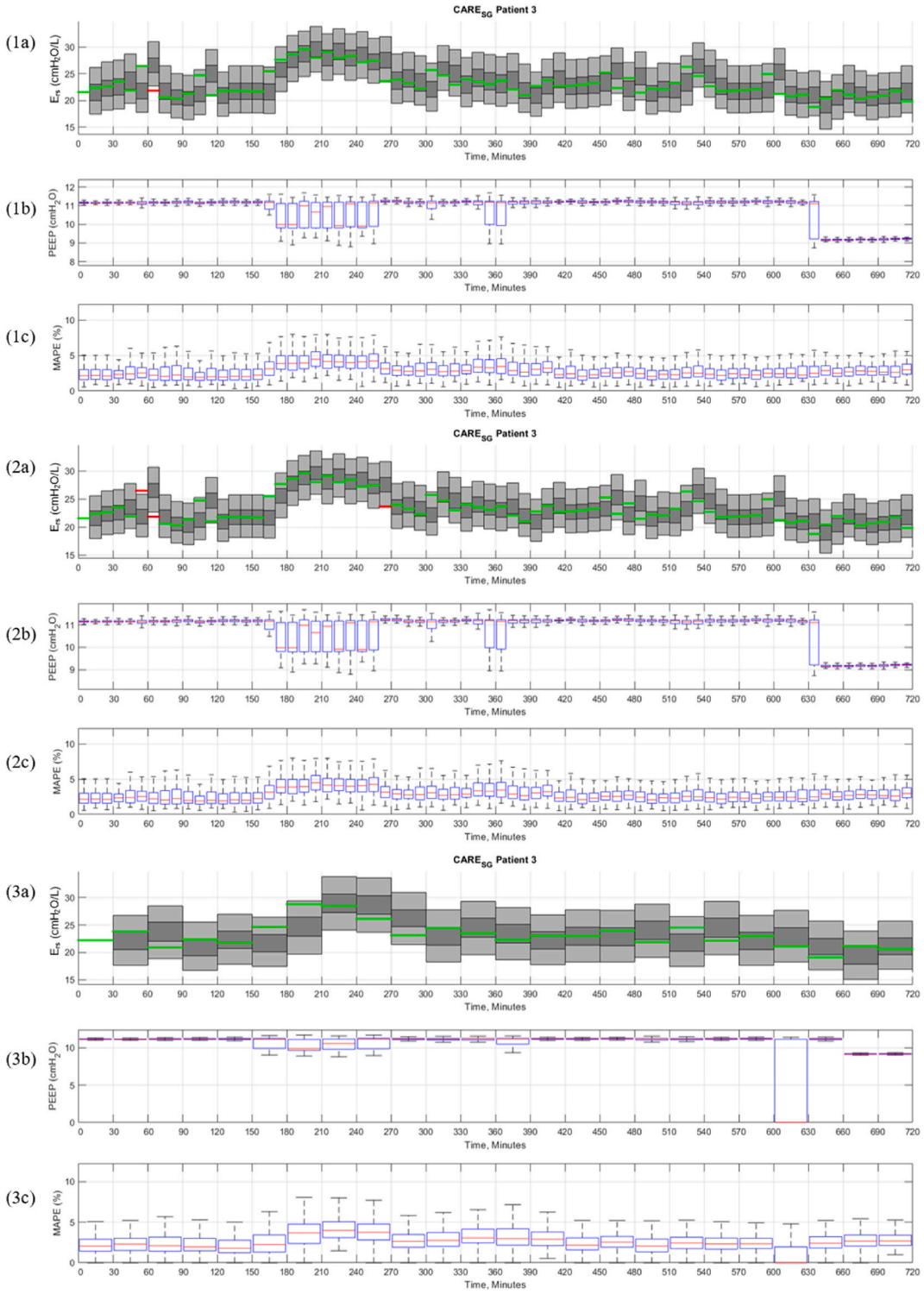

Fig. 6. Analysis of $CARE_{SG}$ Patient 3 using: SM1 (1a, 1b, 1c), SM2 (2a, 2b, 2c), and SM3 (3a, 3b, 3c). Patient E_{rs} profiles and the stochastic model predicted $E_{rs,N+1}$ range are shown in panels 1a, 2a, and 3a. Actual $E_{rs,N+1}$ values which fall within and outside of the stochastic model predicted $E_{rs,N+1}$ 5th – 95th percentiles are plotted in green and red, respectively. The patient PEEP levels are shown in panels 1b, 2b, and 3b. The MAPE of model fitting is presented in panels 1c, 2c, and 3c.

density of $E_{rs\ N}$ for SM1, SM2, and SM3 respectively. It is observed that for values of $E_{rs\ N}$ less than 75 cmH_2O/L, there is a relatively higher probability density, marked by the regions of yellow-coloured peaks. This trend is due to the datapoint density is higher in the regions of $E_{rs\ N}$ less than 75 cmH_2O/L as shown in the plots of Fig. 5. In SM2, an increase in the training dataset size and thus datapoint density, results in tighter percentile lines throughout the range of $E_{rs\ N}$, especially in the range of $E_{rs\ N} > 75$ cmH_2O/L. This shows patients in the $CARE_{02}$ cohort have a wider range of E_{rs} as seen in Fig. 2, thus contributing to data points of higher E_{rs}.

The tighter percentile lines of SM2 relative to SM1 also show an increase in training dataset size along with increased patient variability, leading to an improvement in stochastic model performance in terms of both range and predictive accuracy. For SM3, the percentile lines are

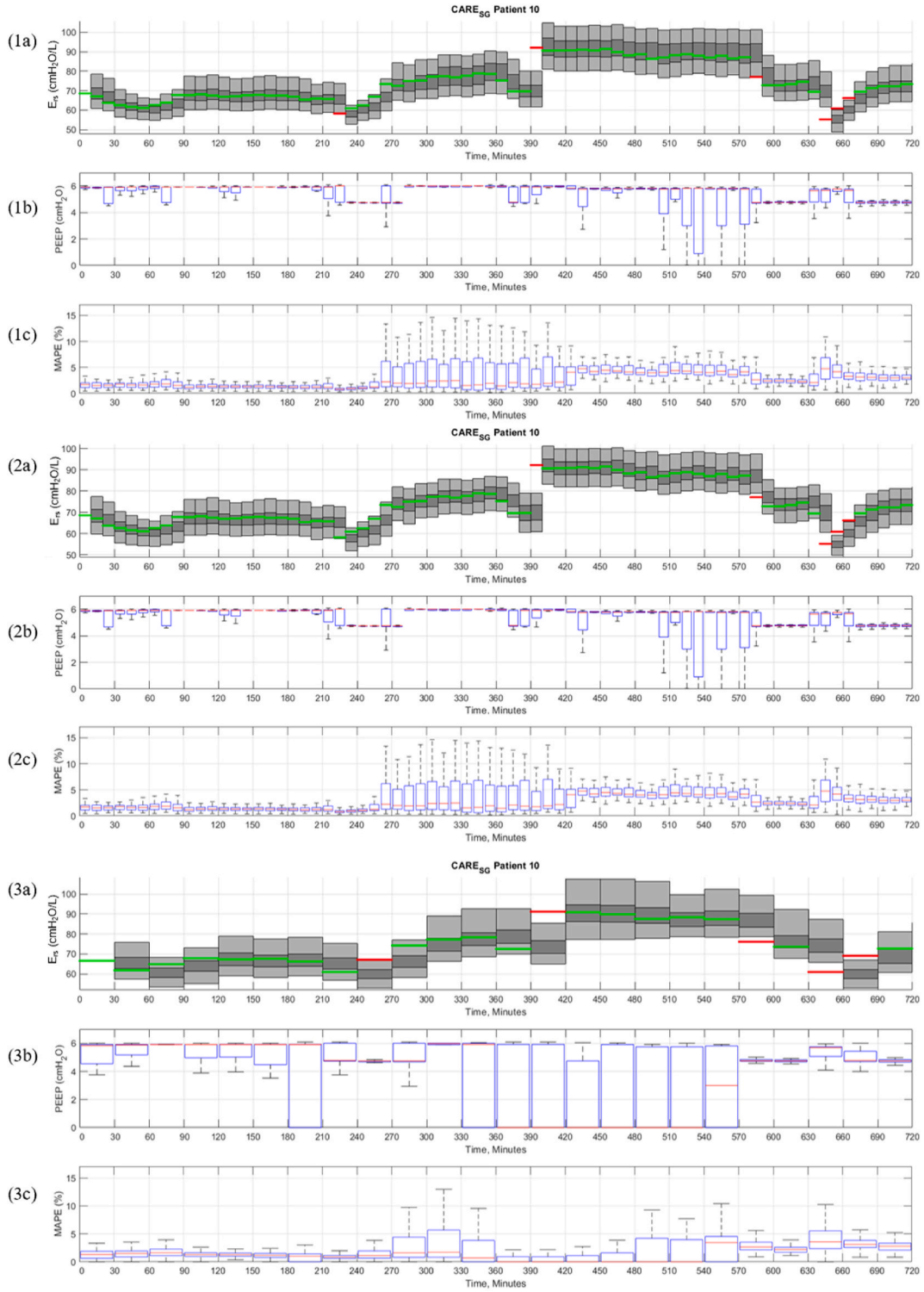

Fig. 7. Analysis of CARE$_{SG}$ Patient 10 using: SM1 (1a, 1b, 1c), SM2 (2a, 2b, 2c), and SM3 (3a, 3b, 3c). Patient E_{rs} profiles and the stochastic model predicted $E_{rs,N+1}$ range are shown in panels 1a, 2a, and 3a. Actual $E_{rs,N+1}$ values which fall within and outside of the stochastic model predicted $E_{rs,N+1}$ 5th – 95th percentiles are plotted in green and red, respectively. The patient PEEP levels are shown in panels 1b, 2b, and 3b. The MAPE of model fitting is presented in panels 1c, 2c, and 3c.

wider in comparison to SM1 and SM2. The increased distance between the percentile lines compensates for the greater spread of data over a longer time interval, which is expected as patients have a greater time period in which to change and may thus change more over this time period. However, the sudden vertical jump followed by a horizontal distribution at approximately $E_{rs\ N} = 110$ cmH$_2$O/L observed in Fig. 5e, may be due to reduced data density.

Median clinical E_{rs} of MV patients from the three cohorts in this study, as well as in literature [3,30,50–52], are below 40 cmH$_2$O/L, justifying the sufficiency in $E_{rs\ N}$ range for SM3. In addition, for all stochastic models, the distribution shape of the percentile lines deviates from the expected linear distribution in the $E_{rs\ N}$ range between 0 and 5 cmH$_2$O/L. This behaviour is expected as MV respiratory failure patients tend to have relatively much higher respiratory elastance, leading to

Table 7
Mean absolute percentage difference between stochastic model percentile lines.

Percentile	SM1-SM2	SM1-SM3	SM2-SM3
5th	4.4	2.6	5.2
25th	1.7	1.4	1.9
50th	1.1	1.3	1.1
75th	1.5	1.8	1.6
95th	2.7	2.6	3.5

*SM1-SM2 indicates the comparison between the percentile lines of SM1 and SM2, and so forth.
*Results are reported as mean absolute percentage differences (%).

data scarcity in these lower ranges of $E_{rs\ N}$ as seen in Fig. 2 [30,53]. Therefore, the $E_{rs\ N}$ axis is limited from 5 to 125 cmH_2O during stochastic model comparison analysis.

For self-validation of all 3 stochastic models, approximately 67% and 92% of the actual $E_{rs\ N+1}$ values fall within the 25th – 75th (Pass50) and 5th – 95th (Pass90) percentile range, respectively. Ideally, 50% and 90% of the actual $E_{rs\ N+1}$ values should fall within the respective ranges. Results from the 5-fold cross-validation yield a mean Pass50 of approximately 68% for all 3 models, whereas the mean Pass90 is approximately 90% for SM1, and 92% for both SM2 and SM3. The Pass50 is the model's interquartile range and should cover only 50% of the respiratory elastance. The discrepancy in Pass50 values at 68% from the ideal values of 50% shows the developed stochastic model is a more conservative estimation of the respiratory elastance distribution with higher coverage than it should in this less clinically useful range.

Results from both validation methods are almost similar, with a maximum percentage difference of mean Pass50 and Pass90 of only 1.89% and 3.14%, respectively. This outcome suggests the amount of training data for stochastic model development is sufficient to account for the heterogeneity of respiratory mechanics in the patient cohorts. Both validation methods produce Pass90 results near the ideal values of the 5th – 95th percentile range but show tendencies towards conservative over-estimation. Despite over-estimation in the Pass50 and Pass90 results, it would provide a more conservative predicted respiratory elastance range as more actual $E_{rs\ N+1}$ values fall within the 25–75th and 5–95th percentile ranges, thus providing a higher margin of error during clinical use. The increase in training dataset size is reflected as a lower absolute percentage difference (APD) of the mean Pass90 during cross-validation with respect to the self-validation results. SM2 and SM3 have an APD of 0.20% and 0.19%, respectively, in comparison with the 3.14% of SM1 (benchmark model). This marks an absolute improvement of 2.94% and 2.95% for SM2 and SM3, respectively for the clinically more important prediction of the 90 percentile interval of $E_{rs\ N+1}$ (Pass90).

SM1 and SM2 are developed for a clinically unrealistic prediction interval of 10 min and would lead to a significant increase in clinician workload [27,54]. In the works in glycemic control, insulin interventions are managed on an hourly basis using a stochastic model-integrated protocol (STAR protocol), resulting in improvements to patient care and a reduction in clinician workload [25]. Thus, the development of a 30-min interval stochastic model (SM3) marks a 200% increase in interval length size in comparison to SM1 and SM2. This improvement further bridges the gap towards critical care applications, where clinical assessments and treatment titrations are usually implemented on an hourly basis.

4.2. Clinical validation of stochastic models

Clinical validation of the stochastic models shows SM2 yields a lower percentage of actual $E_{rs\ N+1}$ values that fall within the stochastic model predicted ranges compared to SM1. This result is mainly due to the tighter percentile lines of SM2 where a larger training dataset is used, and thus greater prediction confidence. The $E_{rs\ N+1}$ range prediction of SM3 yields a lower percentage of actual $E_{rs\ N+1}$ values within the predicted 50 percentile interval (median [IQR]: 73.91% [54.35–82.61%]), which suggests a further increase in dataset size may be required for the use of 30 min time intervals, or equally, the first order stochastic model may not be adequate for the size of intra-patient variability seen over this longer time interval. However, the clinically more important prediction of the 90 percentile interval of $E_{rs\ N+1}$ remains good, with a median [IQR] of 100% [96.74–100%] actual $E_{rs\ N+1}$ values falling within this interval.

From the $E_{rs\ N}$ plots in Figs. 6 and 7, the mean values of $E_{rs\ N}$ show fluctuating variations between each 10-min interval. Therefore, by introducing 30-min time intervals, mean $E_{rs\ N+1}$ values would be less affected by the abrupt changes in identified patient E_{rs}. The results in Table 6 show a high percentage of actual $E_{rs\ N+1}$ values fall within the $E_{rs\ N+1}$ intervals predicted by the three stochastic models, with a median of more than 73% and 98% for the 25–75th and 5–95th percentile intervals, respectively. This outcome demonstrates the performance and feasibility of this type of stochastic model for E_{rs} prediction.

Continuous monitoring of patient-specific respiratory mechanics (E_{rs}) or ventilation parameters (PEEP) also allows for the generation of a patient profile for retrospective analysis and tracking of patient disease progression. The time series plots of Patient 3 (Fig. 6) and Patient 10 (Fig. 7) show that patient-specific E_{rs} values evolve dynamically over time. In these plots, the increase in MAPE signifies the presence of patient-specific spontaneous breathing effort. The presence of significant patient respiratory effort could lead to incorrect respiratory parameter identification with the single compartment lung model [29,55,56].

4.3. Comparison of stochastic models

The mean absolute percentage difference (MAPD) between the stochastic model percentile lines for $5 < E_{rs\ N} < 125$ cmH_2O/L are shown in Table 7. There is a relatively higher MAPD (>2.5%) in the comparison of the 5th and 95th percentiles, with the highest MAPD of 5.2% occurring at the 5th percentile in the comparison of SM2 and SM3. This is attributed to the low local data density and non-linear distribution of percentile lines as seen in Fig. 5. However, this maximum MAPD of 5.2% is lower than the maximum MAPD of 5.97% in the works of Uyttendaele et al. which compares the median blood glucose levels, a key performance metric, between two insulin sensitivity stochastic models. This suggests that the percentile lines between the stochastic models SM1, SM2 and SM3 show a relatively low and acceptable magnitude of discrepancy among each other.

A high absolute difference (>0.25) in cumulative distribution density (CDD), particularly at $E_{rs} < 5$ cmH_2O/L and $E_{rs} > 85$ cmH_2O/L is observed in the plots of Fig. 8. The PD_{AUC} which describes the average error per data point over $5 < E_{rs\ N} < 125$ cmH_2O/L, is relatively higher in SM1-SM3 (0.30% and 0.31% more than SM1-SM2 and SM2-SM3, respectively). This is mainly due to the difference in dataset size and time interval between SM1 and SM3. SM1-SM3 and SM2-SM3 have a higher maximum absolute difference in CDD of 0.6195 and 0.7265 respectively, compared to 0.2811 of SM1-SM2. For SM1-SM3 and SM2-SM3, both points of maximum error occur in the range of $105 < E_{rs} < 125$ cmH_2O/L, suggesting that the stochastic models in comparison, have different predictive capabilities in those regions. In other regions where the absolute difference in CDD is low, all three stochastic models offer almost similar predictive capabilities. This further demonstrates that SM3 with a time interval of 30 min is capable of accurate $E_{rs\ N+1}$ predictions in regions of low CDD, with minimal differences from SM1 and SM2. The feasibility of a 30-min stochastic model thus provides additional clinical utility, potentially improving patient care without adding significant clinical burden to intensive care units.

4.4. Future work

Adding the $CARE_{02}$ cohort to the training dataset extended the useful

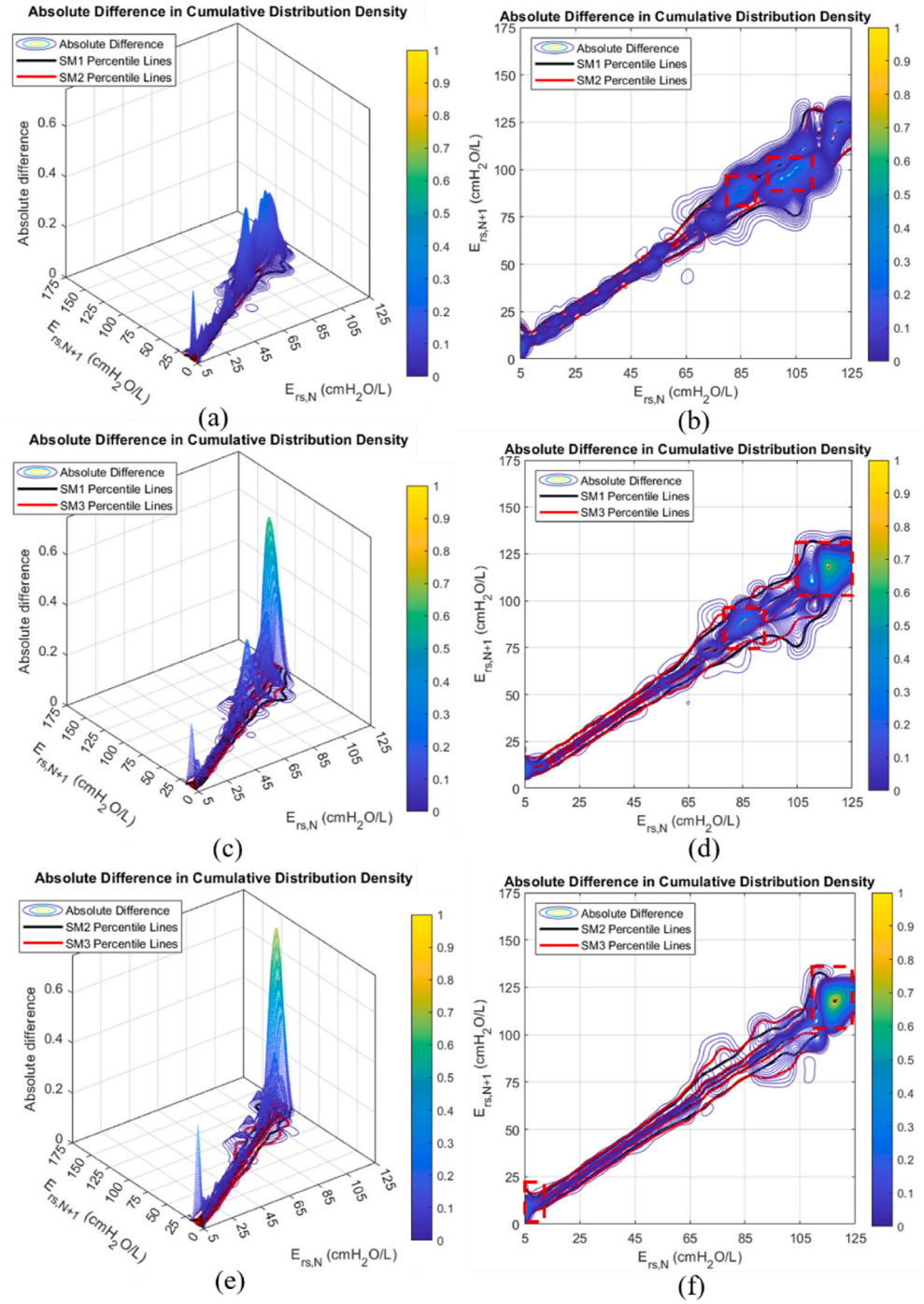

Fig. 8. The orthogonal view (left column) and top view (right column) of the absolute difference in CDD plots. From top to bottom: (a,b): SM1 vs SM2, (c,d): SM1 vs SM3, (e,f): SM2 vs SM3. The maximum absolute difference in CDD is 0.2811, 0.6195, and 0.7265 (from top to bottom). The PD_{AUC} are 1.16%, 1.46% and 1.15% (from top to bottom). The regions of higher absolute difference (>25%) are highlighted by the red dashed rectangles.

$E_{rs\ N}$ prediction range. However, longer time intervals, such as that of SM3 exhibit data scarcity at higher ranges of $E_{rs\ N}$ as each time interval tends to be saturated with lower E_{rs} values, indicating a non-Gaussian distribution of E_{rs} values within an interval, which is also evident in the overall histograms of Fig. 2. This result suggests more data may be necessary to achieve sufficient data density at higher $E_{rs\ N}$ ranges and longer prediction intervals.

One possible method of reducing overestimation in the 25th – 75th or 5th – 95th percentiles and narrower ranges is shown in the works of Le Compte et al., where a constant is introduced to vary the local variance estimator [22]. Thus, it would be possible to produce tighter model percentile lines, but with a less smooth probability distribution, potentially bringing Pass50 and Pass90 closer to their ideal values. In this study, the constant is unmodified as to provide a fair comparison with the stochastic model previously developed by Lee et al. [7]. Therefore, this approach leads to the discrepancy in Pass50 values between the obtained results and the ideal value of 50%.

The single compartment lung model used is easily identifiable but can be inaccurate when significant patient spontaneous breathing is present. The use of better respiratory models [34,40,55–57] capable of capturing and modelling patient respiratory effort could ameliorate this issue. Some of these models also enable direct calculation of

patient-specific and breath-to-beath work of breathing, and thus ventilator unloading in comparison to the work done by the ventilator, which is clinically meaningful in assisted breathing modes [58]. Managing this issue would allow extension towards more assisted spontaneous breathing modes of MV, as well.

Other future works include exploring more clinical trials in different centers where more data can be collected using a network data acquisition and monitoring system for the further development of the stochastic models [42,59]. In addition, mechanical ventilation virtual patients could also serve as a platform for safely and virtually validating the developed stochastic models [60]. A dedicated virtual patient platform where patient profiles consisting of patient-specific sensitivities such as respiratory elastance could enable the testing of a stochastic model-based protocol, thus allowing the long-term performance validation of the stochastic models.

5. Conclusions

In this study, two stochastic models with time intervals of 10 and 30 min respectively, were developed using patient-specific respiratory elastance from two clinical cohorts. When compared to a model from a benchmark study, the larger training dataset enabled tighter stochastic model percentile lines, increased effective prediction range and more robust prediction. The models were validated using retrospective data from an independent patient cohort, with a median of more than 98% of actual $E_{rs\ N+1}$ values falling within the model-predicted 5th – 95th percentile range for all models, confirming robust prediction ability. A comparison of the stochastic models shows similar predictive capabilities in the range of $5 < E_{rs} < 85$ cmH_2O/L, even when a time interval of 30 min is used. The improved stochastic models improve the clinical utility, and thus feasibility for synchronisation with clinical ICU interventions.

Declaration of competing interest

None declared.

Acknowledgements

This research did not receive any specific grant from funding agencies in the public, commercial, or not-for-profit sectors.

References

[1] V.J. Major, Y.S. Chiew, G.M. Shaw, J.G. Chase, Biomedical engineer's guide to the clinical aspects of intensive care mechanical ventilation, Biomed. Eng. Online 17 (2018) 169.
[2] R.G. Brower, M.A. Matthay, A. Morris, D. Schoenfeld, B.T. Thompson, A. Wheeler, Ventilation with lower tidal volumes as compared with traditional tidal volumes for acute lung injury and the acute respiratory distress syndrome, N. Engl. J. Med. 342 (2000) 1301–1308.
[3] M. Briel, M. Meade, A. Mercat, R.G. Brower, D. Talmor, S.D. Walter, A.S. Slutsky, E. Pullenayegum, Q. Zhou, D. Cook, L. Brochard, J.C. Richard, F. Lamontagne, N. Bhatnagar, T.E. Stewart, G. Guyatt, Higher vs lower positive end-expiratory pressure in patients with acute lung injury and acute respiratory distress syndrome: systematic review and meta-analysis, JAMA 303 (2010) 865–873.
[4] M.B.P. Amato, M.O. Meade, A.S. Slutsky, L. Brochard, E.L.V. Costa, D. A. Schoenfeld, T.E. Stewart, M. Briel, D. Talmor, A. Mercat, J.-C.M. Richard, C.R. R. Carvalho, R.G. Brower, Driving pressure and survival in the acute respiratory distress syndrome, N. Engl. J. Med. 372 (2015) 747–755.
[5] P.L. Silva, P.R.M. Rocco, The basics of respiratory mechanics: ventilator-derived parameters, Ann. Transl. Med. 6 (2018) 376, 376.
[6] R. Leong, J.A. Marks, M. Cereda, 10 - how does mechanical ventilation damage lungs? What can be done to prevent it? in: C.S. DEUTSCHMAN, P.J. NELIGAN (Eds.), Evidence-Based Practice of Critical Care, third ed., Elsevier, 2020.
[7] J.W.W. Lee, Y.S. Chiew, X. Wang, C.P. Tan, M.B. Mat Nor, N.S. Damanhuri, J. G. Chase, Stochastic modelling of respiratory system elastance for mechanically ventilated respiratory failure patients, Ann. Biomed. Eng. 49 (2021) 3280–3295.
[8] A.S. Slutsky, V.M. Ranieri, Ventilator-induced lung injury, N. Engl. J. Med. 369 (2013) 2126–2136.
[9] E.J. Van Drunen, Y.S. Chiew, J.G. Chase, B. Lambermont, N. Janssen, T. Desaive, Model-based respiratory mechanics to titrate PEEP and monitor disease state for experimental ARDS subjects, in: 2013 35th Annual International Conference of the IEEE Engineering in Medicine and Biology Society (EMBC), 3-7 July 2013 2013, pp. 5224–5227.
[10] P. Pelosi, L. Ball, C.S.V. Barbas, R. Bellomo, K.E.A. Burns, S. Einav, L. Gattinoni, J. G. Laffey, J.J. Marini, S.N. Myatra, M.J. Schultz, J.L. Teboul, P.R.M. Rocco, Personalized mechanical ventilation in acute respiratory distress syndrome, Crit. Care 25 (2021) 250.
[11] R. Sharma, S.N. Singh, S. Khatri, Medical data mining using different classification and clustering techniques: a critical survey, in: 2016 Second International Conference on Computational Intelligence & Communication Technology (CICT), 2016, pp. 687–691, 12-13 Feb. 2016.
[12] B. Mirkin, Mathematical Classification and Clustering: from How to what and Why, Springer Berlin Heidelberg, Berlin, Heidelberg, 1998, pp. 172–181.
[13] Y. Xiao, Z. Jin, The forecast research of linear regression forecast model in national economy, Open Acess. Lib. J. 8 (2021) 1–17.
[14] T. Székely, K. Burrage, Stochastic simulation in systems biology, Comput. Struct. Biotechnol. J. 12 (2014) 14–25.
[15] D.J. Wilkinson, Stochastic modelling for quantitative description of heterogeneous biological systems, Nat. Rev. Genet. 10 (2009) 122–133.
[16] O. Mejlholm, N. Bøknæs, P. Dalgaard, Development and validation of a stochastic model for potential growth of Listeria monocytogenes in naturally contaminated lightly preserved seafood, Food Microbiol. 45 (2015) 276–289.
[17] D. Kumar, G.S. Murthy, Stochastic molecular model of enzymatic hydrolysis of cellulose for ethanol production, Biotechnol. Biofuels 6 (2013) 63.
[18] A.J. Mckane, T.J. Newman, Stochastic models in population biology and their deterministic analogs, Phys. Rev. 70 (2004), 041902.
[19] L.M. Harrison, O. David, K.J. Friston, Stochastic models of neuronal dynamics, Phil. Trans. Biol. Sci. 360 (2005) 1075–1091.
[20] J. Lin, D. Lee, J.G. Chase, G.M. Shaw, C.E. Hann, T. Lotz, J. Wong, Stochastic modelling of insulin sensitivity variability in critical care, Biomed. Signal Process Control 1 (2006) 229–242.
[21] J. Lin, D. Lee, J.G. Chase, G.M. Shaw, A. Le Compte, T. Lotz, J. Wong, T. Lonergan, C.E. Hann, Stochastic modelling of insulin sensitivity and adaptive glycemic control for critical care, Comput. Methods Progr. Biomed. 89 (2008) 141–152.
[22] A.J. Le Compte, D.S. Lee, J.G. Chase, J. Lin, A. Lynn, G.M. Shaw, Blood glucose prediction using stochastic modeling in neonatal intensive care, IEEE Trans. Biomed. Eng. 57 (2010) 509–518.
[23] M. Capan, J.S. Ivy, J.R. Wilson, J.M. Huddleston, A stochastic model of acute-care decisions based on patient and provider heterogeneity, Health Care Manag. Sci. 20 (2017) 187–206.
[24] V. Uyttendaele, J.L. Knopp, S. Davidson, T. Desaive, B. Benyo, G.M. Shaw, J. G. Chase, 3D kernel-density stochastic model for more personalized glycaemic control: development and in-silico validation, Biomed. Eng. Online 18 (2019) 102.
[25] L.M. Fisk, A.J. Le Compte, G.M. Shaw, S. Penning, T. Desaive, J.G. Chase, STAR development and protocol comparison, IEEE Trans. Biomed. Eng. 59 (2012) 3357–3364.
[26] V. Uyttendaele, J.L. Knopp, M. Pirotte, P. Morimont, B. Lambermont, G.M. Shaw, T. Desaive, J.G. Chase, STAR-liège clinical trial interim results: safe and effective glycemic control for all, Annu. Int. Conf. IEEE Eng. Med. Biol. Soc. 2019 (2019) 277–280.
[27] P. Guo, Y.S. Chiew, G.M. Shaw, L. Shao, R. Green, A. Clark, J.G. Chase, Clinical Activity Monitoring System (CATS): an automatic system to quantify bedside clinical activities in the intensive care unit, Intensive Crit. Care Nurs. 37 (2016) 52–61.
[28] F. Vicario, A. Albanese, N. Karamolegkos, D. Wang, A. Seiver, N.W. Chbat, Noninvasive estimation of respiratory mechanics in spontaneously breathing ventilated patients: a constrained optimization approach, IEEE Trans. Biomed. Eng. 63 (2016) 775–787.
[29] Y.S. Chiew, C. Pretty, P.D. Docherty, B. Lambermont, G.M. Shaw, T. Desaive, J. G. Chase, Time-varying respiratory system elastance: a physiological model for patients who are spontaneously breathing, PLoS One 10 (2015), e0114847.
[30] D.R. Hess, Respiratory mechanics in mechanically ventilated patients, Respir. Care 59 (2014) 1773.
[31] A.R. Carvalho, W.A. Zin, Respiratory system dynamical mechanical properties: modeling in time and frequency domain, Biophys Rev. 3 (2011) 71.
[32] Y.S. Chiew, J.G. Chase, G. Arunachalam, C.P. Tan, N.L. Loo, Y.W. Chiew, A. M. Ralib, M.B. Mat Nor, Clinical application of respiratory elastance (care trial) for mechanically ventilated respiratory failure patients: a model-based study, IFAC-PapersOnLine 51 (2018) 209–214.
[33] K.T. Kim, J. Knopp, B. Dixon, G. Chase, Quantifying neonatal pulmonary mechanics in mechanical ventilation, Biomed. Signal Process Control 52 (2019) 206–217.
[34] D.P. Redmond, Y.S. Chiew, V. Major, J.G. Chase, Evaluation of model-based methods in estimating respiratory mechanics in the presence of variable patient effort, Comput. Methods Progr. Biomed. 171 (2019) 67–79.
[35] Q. Sun, J.G. Chase, C. Zhou, M.H. Tawhai, J.L. Knopp, K. Möller, S.J. Heines, D. C. Bergmans, G.M. Shaw, Prediction and estimation of pulmonary response and elastance evolution for volume-controlled and pressure-controlled ventilation, Biomed. Signal Process Control 72 (2022), 103367.
[36] P.M. Suter, B. Fairley, M.D. Isenberg, Optimum end-expiratory airway pressure in patients with acute pulmonary failure, N. Engl. J. Med. 292 (1975) 284–289.
[37] Y.S. Chiew, J.G. Chase, G.M. Shaw, A. Sundaresan, T. Desaive, Model-based PEEP optimisation in mechanical ventilation, Biomed. Eng. Online 10 (2011) 111, 111.
[38] M.C. Pintado, R. De Pablo, M. Trascasa, J.M. Milicua, S. Rogero, M. Daguerre, J. A. Cambronero, I. Arribas, M. Sánchez-García, Individualized PEEP setting in

subjects with ARDS: a randomized controlled pilot study, Respir. Care 58 (2013) 1416–1423.
[39] M.E. Cove, M.R. Pinsky, J.J. Marini, Are we ready to think differently about setting PEEP? Crit. Care 26 (2022) 222.
[40] C.Y.S. Ang, Y.S. Chiew, L.H. Vu, M.E. Cove, Quantification of respiratory effort magnitude in spontaneous breathing patients using Convolutional Autoencoders, Comput. Methods Progr. Biomed. 215 (2022), 106601.
[41] A. Szlavecz, Y.S. Chiew, D. Redmond, A. Beatson, D. Glassenbury, S. Corbett, V. Major, C. Pretty, G.M. Shaw, B. Benyo, T. Desaive, J.G. Chase, The Clinical Utilisation of Respiratory Elastance Software (CURE Soft): a bedside software for real-time respiratory mechanics monitoring and mechanical ventilation management, Biomed. Eng. Online 13 (2014).
[42] Q.A. Ng, Y.S. Chiew, X. Wang, C.P. Tan, M.B. Mat Nor, N.S. Damanhuri, J.G. Chase, Network Data Acquisition and Monitoring System for Intensive Care Mechanical Ventilation Treatment, IEEE Access, 2021, p. 1, 1.
[43] V. Major, S. Corbett, D.P. Redmond, A. Beatson, D. Glassenbury, Y.S. Chiew, C. G. Pretty, T. Desaive, Á. Szlávecz, B. Benyó, G.M. Shaw, J.G. Chase, Respiratory Mechanics Assessment for Reverse-Triggered Breathing Cycles Using Pressure Reconstruction, Biomedical Signal Processing and Control, 2016.
[44] J.H. Bates, Lung Mechanics: an Inverse Modeling Approach, Cambridge University Press, 2009.
[45] E.J. Van Drunen, Y.S. Chiew, C. Pretty, G.M. Shaw, B. Lambermont, N. Janssen, J. G. Chase, T. Desaive, Visualisation of time-varying respiratory system elastance in experimental ARDS animal models, BMC Pulm. Med. 14 (2014) 33.
[46] A. Gramacki, Nonparametric Kernel Density Estimation and its Computational Aspects, Springer International Publishing, Cham, Switzerland, 2018.
[47] J.W.W. Lee, Y.S. Chiew, C.P. Tan, A.A. Razak, N.N. Abdul Razak, Analysis of insulin sensitivity stochastic models between STAR original and Malaysian cohorts, IFAC-PapersOnLine 53 (2020) 16143–16148.
[48] M.B. Amato, C.S. Barbas, D.M. Medeiros, R.B. Magaldi, G.P. Schettino, G. Lorenzi-Filho, R.A. Kairalla, D. Deheinzelin, C. Munoz, R. Oliveira, T.Y. Takagaki, C. R. Carvalho, Effect of a protective-ventilation strategy on mortality in the acute respiratory distress syndrome, N. Engl. J. Med. 338 (1998) 347–354.
[49] L. Papazian, C. Aubron, L. Brochard, J.-D. Chiche, A. Combes, D. Dreyfuss, J.-M. Forel, C. Guérin, S. Jaber, A. Mekontso-Dessap, A. Mercat, J.-C. Richard, D. Roux, A. Vieillard-Baron, H. Faure, Formal guidelines: management of acute respiratory distress syndrome, Ann. Intensive Care 9 (2019) 69.
[50] Y.S. Chiew, C.G. Pretty, G.M. Shaw, Y.W. Chiew, B. Lambermont, T. Desaive, J. G. Chase, Feasibility of titrating PEEP to minimum elastance for mechanically ventilated patients, Pilot. Feasibility. Stud. 1 (2015) 9.
[51] R.G. Brower, Higher versus lower positive end-expiratory pressures in patients with the acute respiratory distress syndrome, N. Engl. J. Med. 351 (2004) 327–336.
[52] Y.S. Chiew, J.G. Chase, G.M. Shaw, T. Desaive, Respiratory system elastance monitoring during PEEP titration, Crit. Care 16 (2012) P103.
[53] D.C. Grinnan, J.D. Truwit, Clinical review: respiratory mechanics in spontaneous and assisted ventilation, Crit. Care 9 (2005) 472–484.
[54] V. Uyttendaele, J.L. Knopp, G.M. Shaw, T. Desaive, J.G. Chase, Risk and reward: extending stochastic glycaemic control intervals to reduce workload, Biomed. Eng. Online 19 (2020) 1–21.
[55] D.P. Redmond, P.D. Docherty, Y.S. Chiew, J.G. Chase, A polynomial model of patient-specific breathing effort during controlled mechanical ventilation, Annu. Int. Conf. IEEE Eng. Med. Biol. Soc. 2015 (2015) 4532–4535.
[56] C. Zhou, J.G. Chase, Q. Sun, J. Knopp, M.H. Tawhai, T. Desaive, K. Möller, G. M. Shaw, Y.S. Chiew, B. Benyo, Reconstructing asynchrony for mechanical ventilation using a hysteresis loop virtual patient model, Biomed. Eng. Online 21 (2022) 16.
[57] J.L. Knopp, J.G. Chase, K.T. Kim, G.M. Shaw, Model-based Estimation of Negative Inspiratory Driving Pressure in Patients Receiving Invasive NAVA Mechanical Ventilation, Computer Methods and Programs in Biomedicine, 2021, 106300.
[58] E.F.S. Guy, J.G. Chase, J.L. Knopp, G.M. Shaw, Quantifying ventilator unloading in CPAP ventilation, Comput. Biol. Med. 142 (2022), 105225.
[59] Q.A. Ng, C.Y.S. Ang, Y.S. Chiew, X. Wang, C.P. Tan, M.B.M. Nor, N.S. Damanhuri, J.G. Chase, CAREDAQ: data acquisition device for mechanical ventilation waveform monitoring, HardwareX 12 (2022), e00358.
[60] C.Y.S. Ang, J.W.W. Lee, Y.S. Chiew, X. Wang, C.P. Tan, M.E. Cove, M.B. Mat Nor, C. Zhou, T. Desaive, J.G. Chase, Virtual Patient Framework for the Testing of Mechanical Ventilation Airway Pressure and Flow Settings Protocol, Computer Methods and Programs in Biomedicine, 2022, 107146.